CHAPTER IV
RESULTS AND DISCUSSION

4.1 The Effect Flow Rate on the Scallop Surface

Two different flow rates providing two different Reynolds numbers at room temperature (25°C) were studied in plaster conduits. After each run, the test sections were removed from the test loop to characterise the plaster surface by photography and the liquid samples were analysed to obtain the dissolution rates vs time.

4.1.1 Scallop Surface

It was found that the entrance of a conduit has a thinner wall than the exit. This may result from higher turbulence within the entrance length, as shown in Figure 4.1.

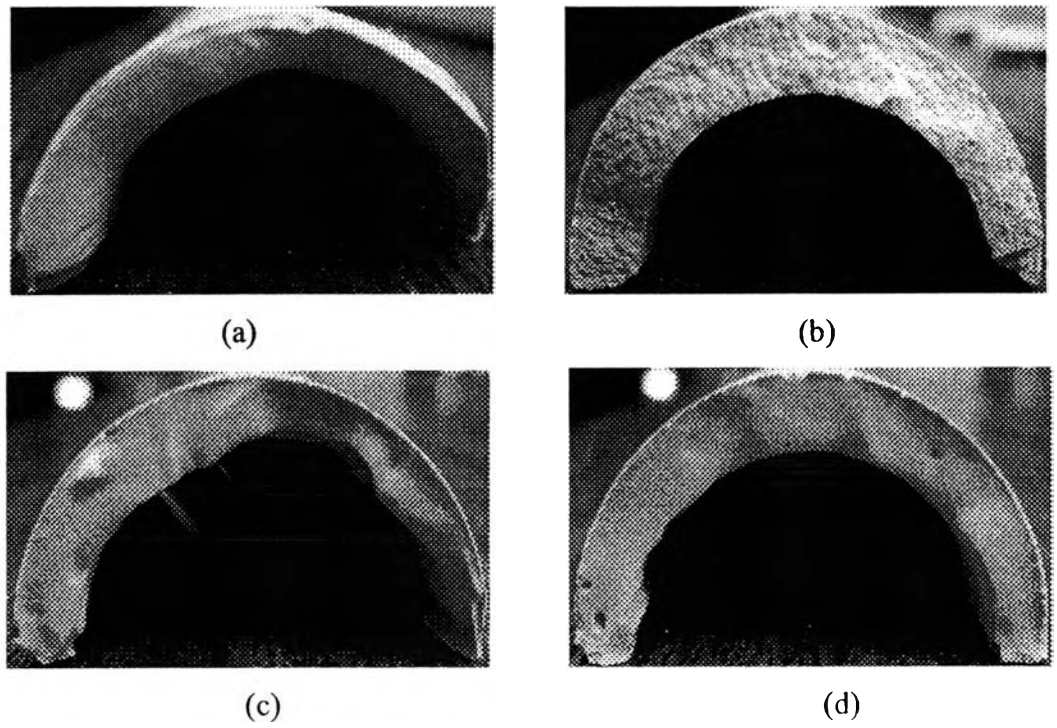

Figure 4.1 Plaster test sections at different positions (a) 25 LPM at the entrance, (b) 25 LPM at the exit, (c) 35 LPM at the entrance, (d) 35 LPM at the exit

Moreover, the scallop surface at the inlet and outlet are different. From Figure 4.2, it shows that at the inlet smaller scallops occur but with a higher population than the outlet. This is probably caused by the higher turbulence at the inlet.

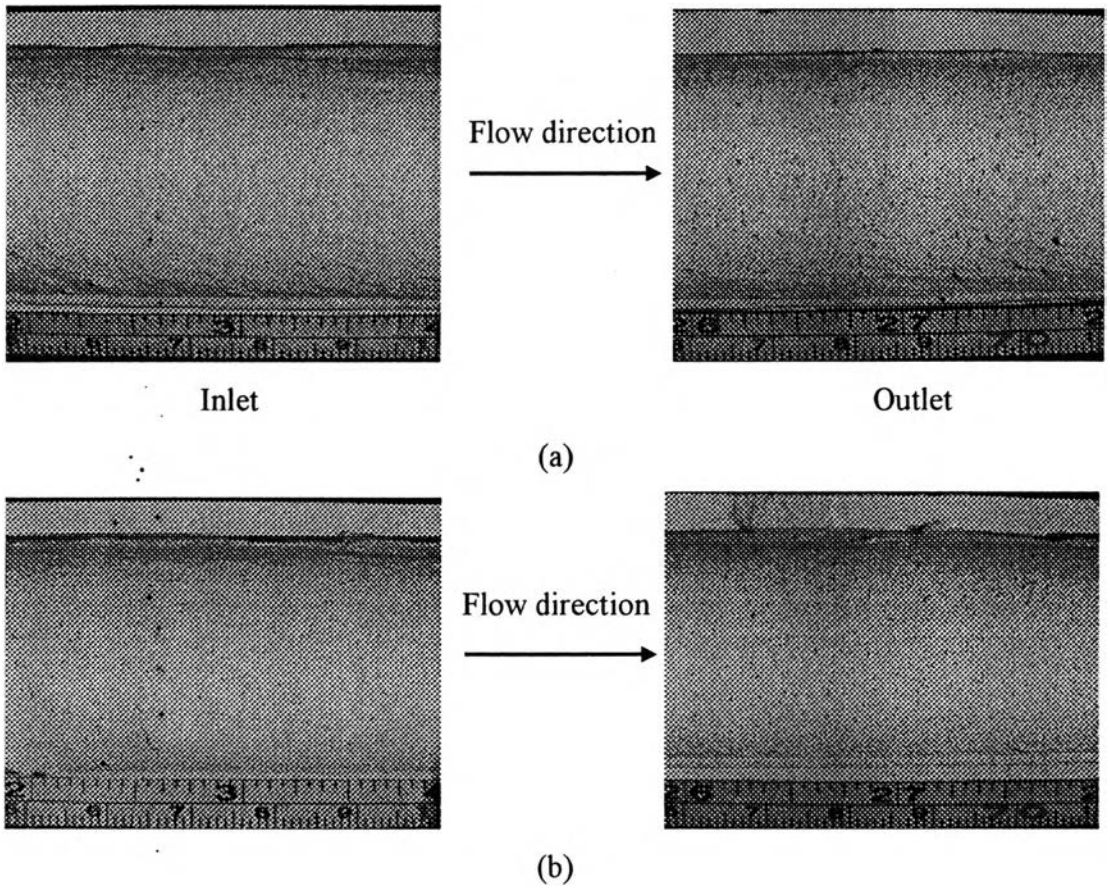

Figure 4.2 Plaster test sections after experimental runs at different flow rates (a) at 35 LPM, (b) at 25 LPM

In addition, the water flow rates of 25 LPM and 35 LPM indicated that there was different scalloping. At 25 LPM, scallops spread randomly over the surface and appear to be larger, while at 35 LPM there was a large population of small scallops, as shown in Figure 4.3. The average size of scallops was found to decrease with increasing water flow rate because more scallops overlapped when a similar area is considered. It can be concluded that the population of scallops was observed to develop significantly with increasing water flow rate as higher Reynolds number or higher turbulence occurred at the same time, whereas the average size of the

scallops was found to decrease. It can be concluded that higher turbulence causes different scallops.

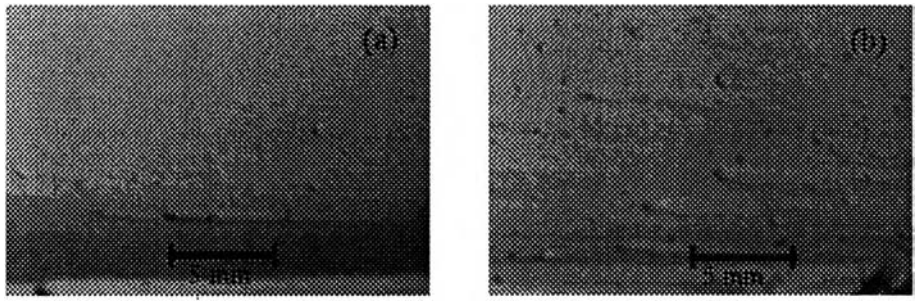

Figure 4.3 Scallop surfaces on the plaster surface after a five-hours run at different flow rates: (a) 25 LPM, $pH_{25°C}$ 7, 25°C and (b) 35 LPM, $pH_{25°C}$ 7, 25 °C

4.1.2 Dissolution Rates

The average dissolution rates of the plaster of Paris were estimated in two ways. Firstly, by measuring the weight of plaster lost by dissolution at the end of the test; this mass loss was transformed to rate of dissolution ($g/m^2.min$). By using the atomic absorption spectrophotometer (AAS) to measure calcium concentration directly, the dissolution rates can be determined at any time.

Two different flow rates, 25 LPM and 35 LPM, were used. This gave Reynolds numbers of 21220 and 29709, respectively. These flow rates were chosen due to the limitation of water flow velocity from taps in the range of Reynolds numbers in previous work. A uniform flow was observed in the conduit, although a slight inlet effect appeared within the first few centimeters of the test section where the turbulence became to be greater.

The experiment was repeated on different types of plaster of Paris at each flow rate. For the first type of plaster (Type I) at 25 LPM and 35 LPM, the dissolution rate increased with time, as shown in Figure 4.4.

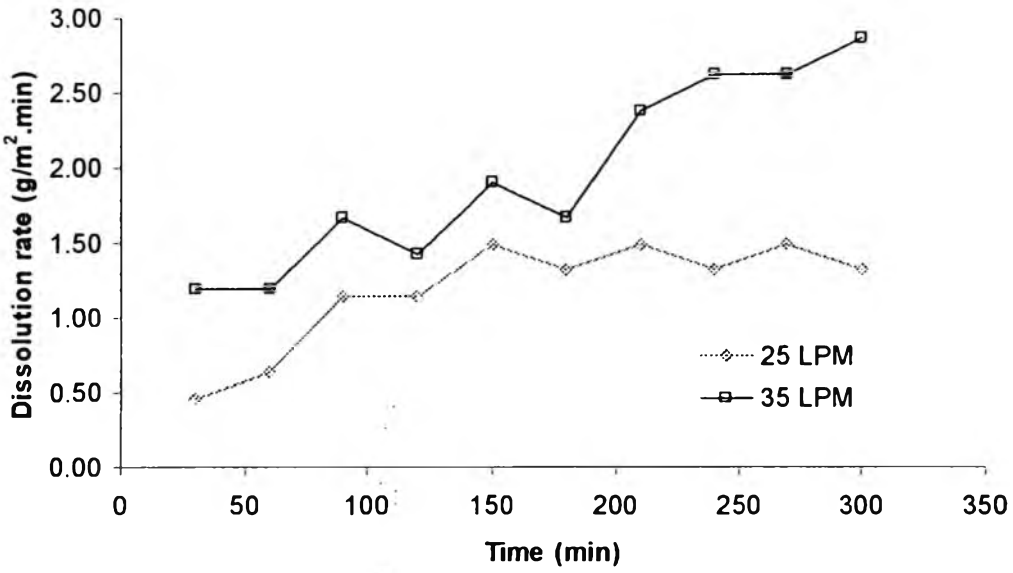

Figure 4.4 Dissolution rate of plaster versus time at different flow rates for Type I, $pH_{25°C}$ 7, 25°C

A second run was made using new type of plaster (Type II) at 35 LPM. From Figure 4.5, it shows to be the same results as Type I, which the dissolution rate increases with time.

From Figure 4.6, the dissolution rate increased with time for third type of plaster (Type III) similar to previous results (Type I and II). One can conclude that the dissolution rate of plaster is proportional to time for any sort of commercial plaster. For all tests, the average dissolution rate increased with flow rate. The dissolution rate at 35 LPM was higher than at 25 LPM.

For any type of plaster, the dissolution rates increase in given time because of increasing plaster surface. Moreover, the different flow rates present different dissolution rates. This indicates that diffusion transport is the limiting step because the dissolution rates increase with the flow rate. However, the dissolution rates should increase in a uniform pattern when the Reynolds number increases if the diffusion transport exclusively controls. It seems that there is another mechanism controlling the dissolution rates since the dissolution rates after three hours change to a higher rate. The surface reaction and the increasing plaster surface may be the cause of this change in dissolution rate.

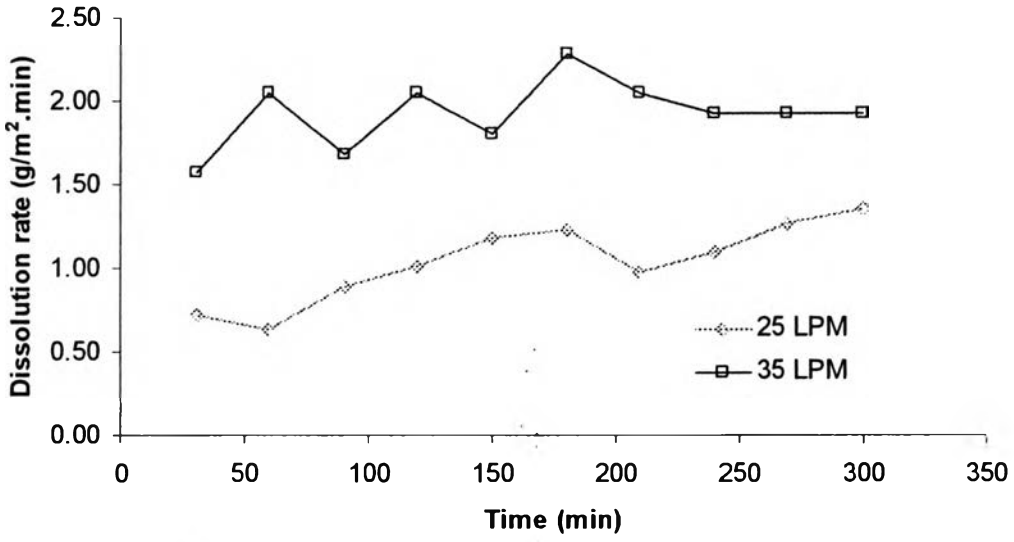

Figure 4.5 Dissolution rate of plaster versus time at different flow rates in Type II, $pH_{25°C}$ 7, 25°C

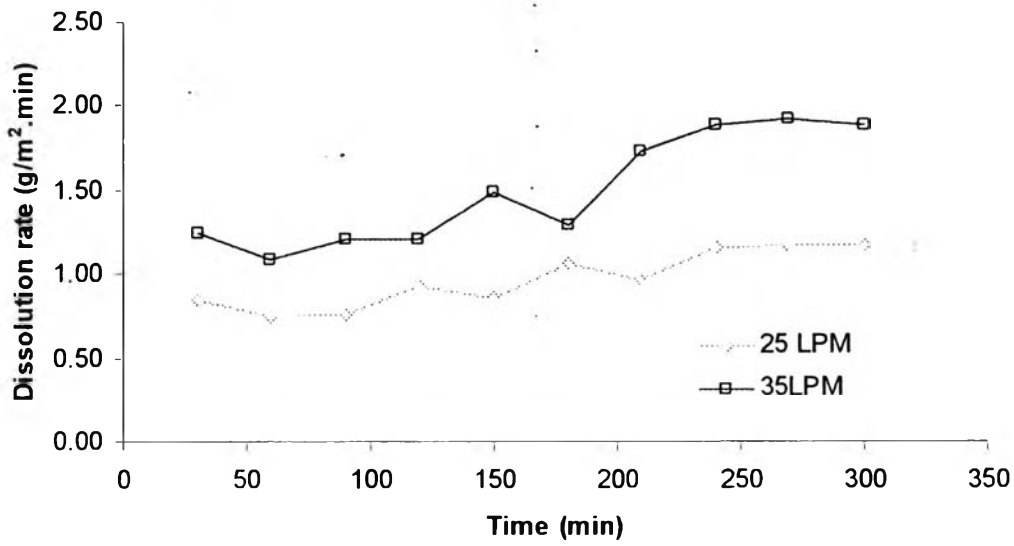

Figure 4.6 Dissolution rate of plaster versus time at different flow rates in Type III $pH_{25°C}$ 7, 25°C

4.2 The Effect pH on the Scallop Surface

The two different flow rates were studied at three different pHs (pH = 3, 7 and 10) at 25°C by using nitric acid and sodium hydroxide to control the pH.

4.2.1 Scallop Surface

After each run, the plaster conduits were photographed to characterise the scallop surface. At the low flow rate, the population of scallops at pH 3 is higher than at pH 7 and 10, as shown in Figure 4.7(a1), (b1) and (c1). The population of scallops shows to decrease with increasing pH. At the high flow rate, however, the population of scallops shows similar at pH 3, 7 and 10, as shown in Figure 4.7(a2), (b2) and (c2). Therefore, the flow rate affects the formation of scallops significantly more than pH. The water chemistry may influence the scalloping once the process has started.

From observing the scallops at any time, at pH 3 and low flow rate, the scallops show to start developing after two hours and then the population of scallops continuously increases, as shown in Figure 4.8(a1-5). At the high flow rate, the initial scallops were formed after 30 minutes and the population of scallops continuously increased, as shown in Figure 4.9(a1-5). This indicates that the initiation of scallops starts at the high flow rate faster than at the low flow rate. This causes the population of scallops to be higher at the high flow rate.

At pH 7 and the low flow rate, the scallops start to develop after two hours the same as for pH 3 and then the population of scallops increased similar for pH 3, as shown in Figure 4.8(b1-5). At the high flow rate, the scalloping occurs after 1½ hours and then continuously increases, as shown in Figure 4.9(b1-5).

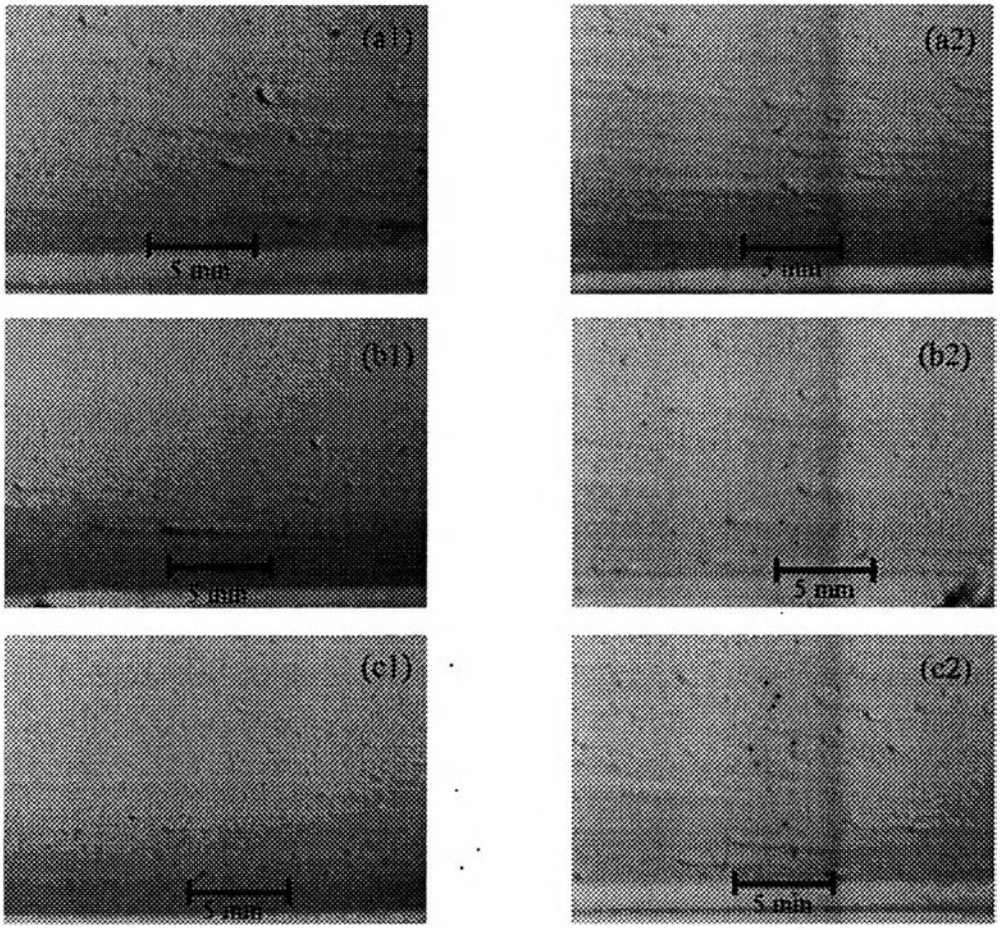

Figure 4.7 The scallop surfaces on the plaster surface after run under different conditions: (a1) $pH_{25°C}$ 3, 25 LPM, (b1) $pH_{25°C}$ 7, 25 LPM, (c1) $pH_{25°C}$ 10, 25 LPM, (a2) $pH_{25°C}$ 3, 35 LPM, (b2) $pH_{25°C}$ 7, 35LPM and (c2) $pH_{25°C}$ 10, 35 LPM

At pH 10 and the low flow rate, the scallops start to develop after two hours similar to the situation at pH 3 and then the population of scallops increased with time, as shown in Figure 4.8(c1-5). At the high flow rate, the scallops were initially formed after 1½ hours and continuously increased, as shown in Figure 4.9 (c1-5). Due to the late initiation of scalloping at pH 10, the population of scallops at pH 10 is less than at pH 3 and 7. It can be concluded that the water chemistry may influence the initiation of scalloping.

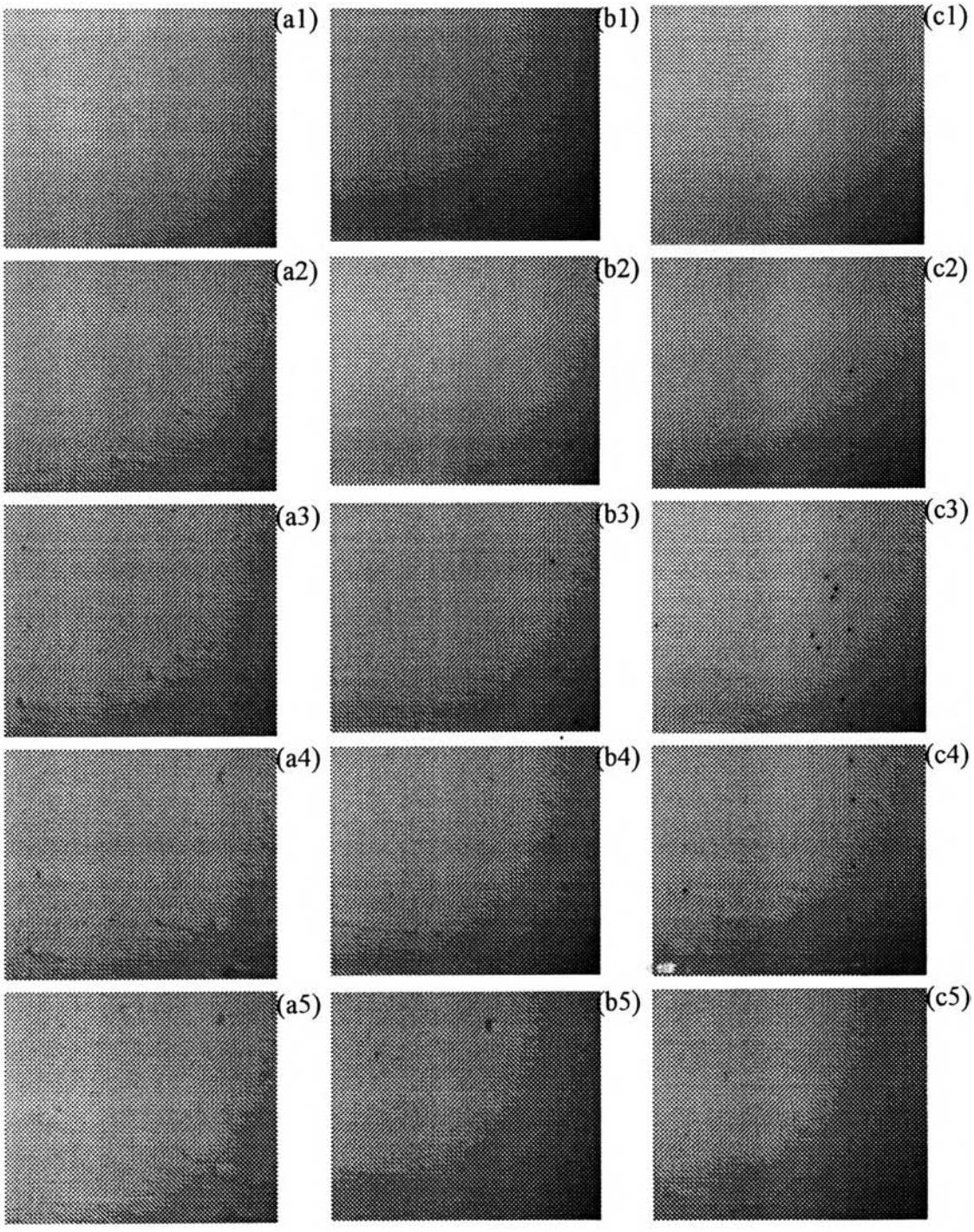

Figure 4.8 The scallop surface developing every one hour at 25 LPM under different conditions: (a1-5) $pH_{25°C}$ 3, (b1-5) $pH_{25°C}$ 7 and (c1-5) $pH_{25°C}$ 10

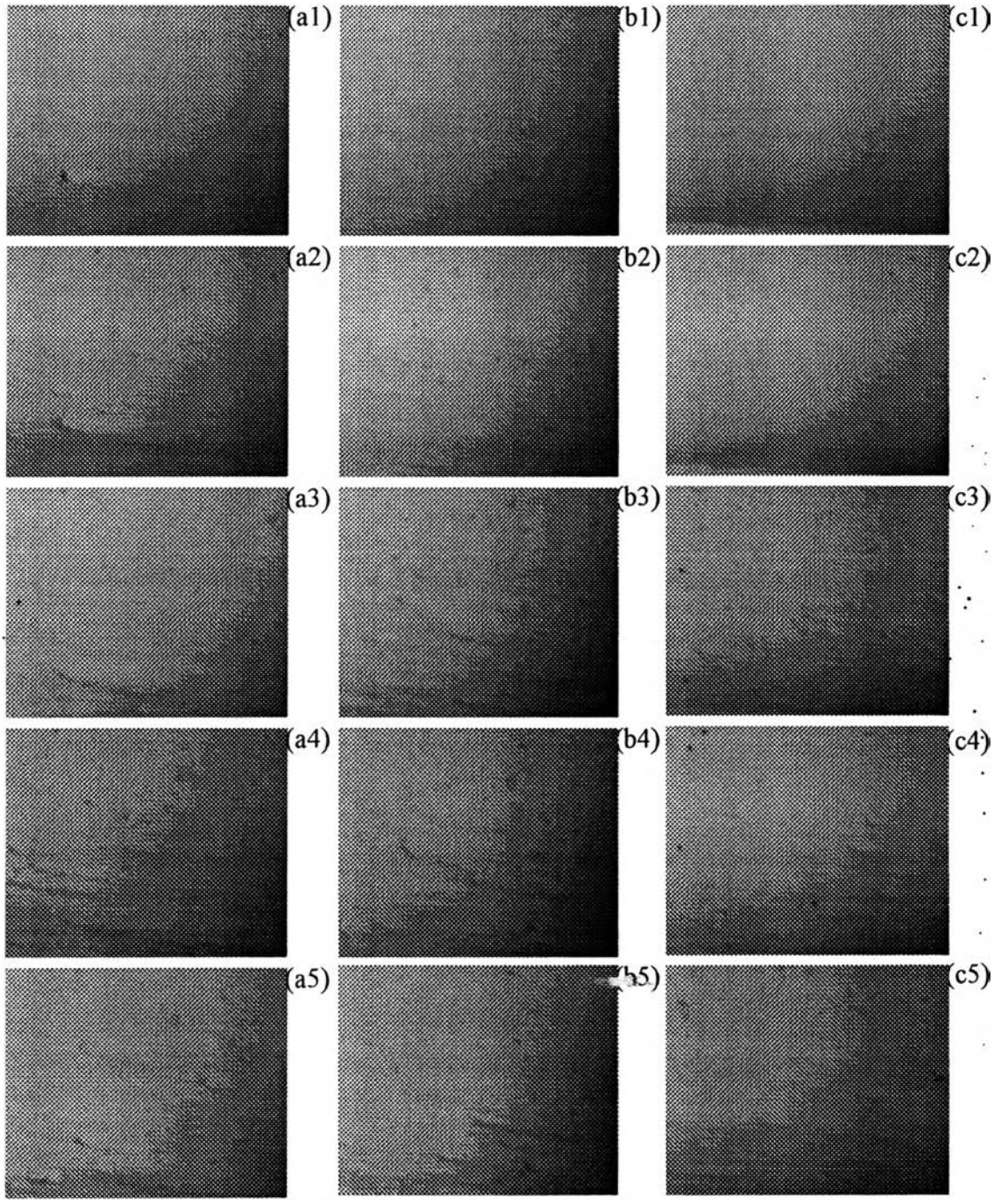

Figure 4.9 The scallop surface developing every one hour at 35 LPM under different conditions: (a1-5) $pH_{25^{\circ}C}$ 3, (b1-5) $pH_{25^{\circ}C}$ 7 and (c1-5) $pH_{25^{\circ}C}$ 10

4.2.3 Dissolution Rates

From the results at pH 3, the dissolution rates show to increase after a certain time, as shown in Figure 4.10. Similar results were found at pH 7, as shown in Figure 4.6. For a pH 3, however, the dissolution rate was high at the beginning of the experiment and drops to about a half of the initial value after 30 minutes. The dissolution rate again increases after one hour and remains stable after four hours.

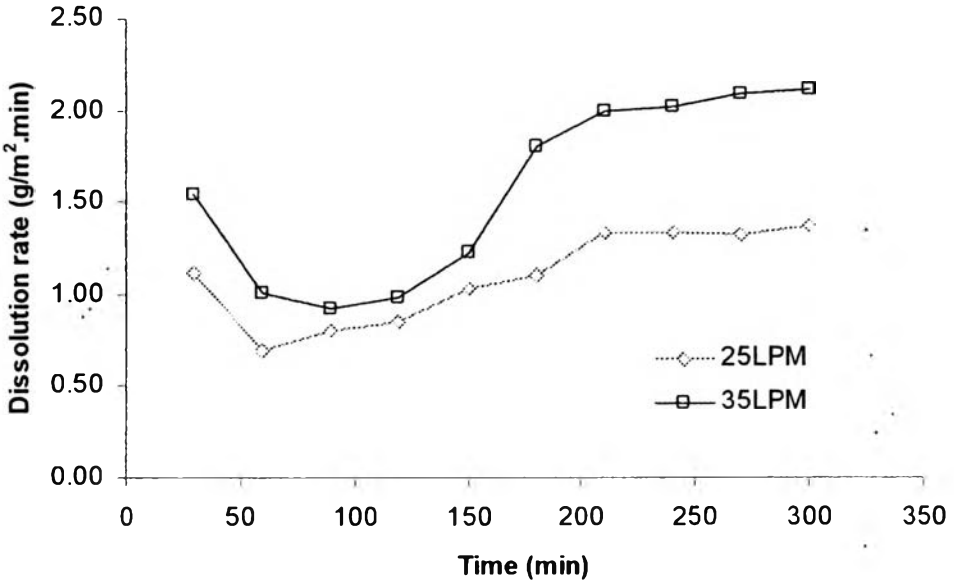

Figure 4.10 The dissolution rate versus time at $pH_{25°C}$ 3, 25°C

The dissolution rate is high at the beginning of the experiment because the plaster test section had dried. It was therefore easily dissolved into the solution. The dissolution rate drops when the plaster section has totally absorbed the solution at the constant surface area. This leads to a decrease of the dissolution rate after 30 minutes or earlier. As the process continues, the plaster surface will increase and this causes the dissolution rate becomes to increase after the initial reduction. The formation of scallops causes the plaster surface to increase as time passes. The surface area becomes greater and increases the dissolution rate. A high flow rate will cause an increasing dissolution rate. The difference of dissolution rates between the high and low flow rates are stable until the surface area increases after three hours.

The dissolution rate of plaster or gypsum is controlled by the diffusion transport under this condition. The dissolution rate increases with increasing flow rate and it will increase if the surface area becomes greater.

From the results of pH 10, the dissolution rate decreases with time, as shown in Figure 4.11, which it is significantly different from pH 3 and 7 results. The dissolution rate is very high at the beginning and decreases for 1-2 hours after which it becomes stable.

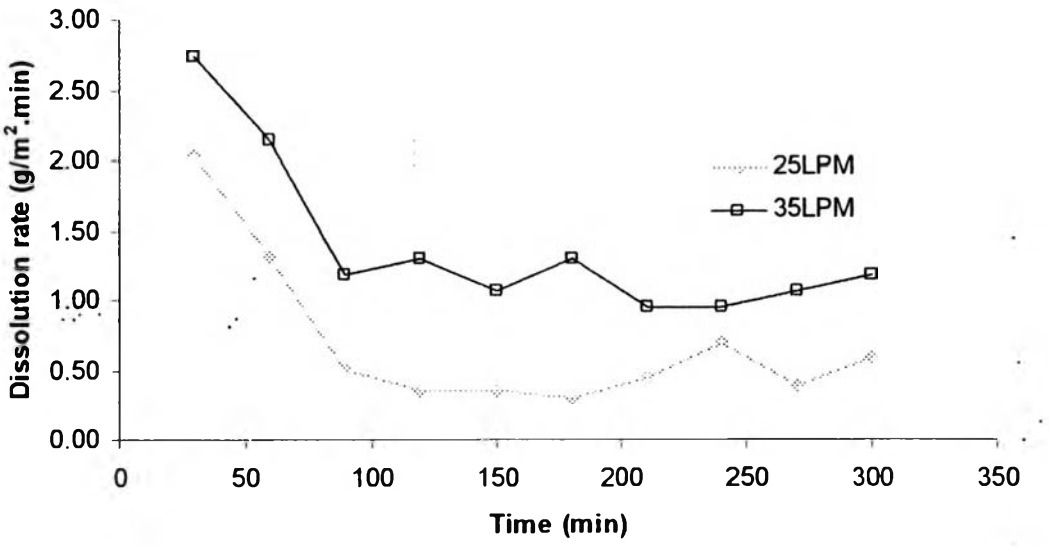

Figure 4.11 The dissolution rate versus time at $pH_{25°C}$ 10, 25°C

The dissolution rate of plaster is high at the beginning of the experiment as for the two previous two conditions. It results from the dried plaster test section. The dissolution rate decreases instead of increasing with increasing surface area. In this case, the surface area has less effect on the dissolution rate. . It is possible that some compound of the solution forms and precipitates on the surface and the coated surface becomes insoluble. Other mechanisms may also be involved in the decrease of plaster dissolution rate with time. After nearly two hours, the dissolution rate becomes stable and slightly increases after four hours. This is because of the developing of scallops on the plaster surface.

In this case, the dissolution rate decreases with time which it is different results from occurring at pH 7 and 3. It postulates that the surface area has less effect

on the dissolution rate. From observation on the experiment, it appeared some unknown particles deposit on the sample tubes after run. Therefore, it is possible that the solution reacted the surface and formed the chemical compound to precipitates on the surface and the coated surface becomes insoluble.

At pH 10, the dissolution rate of plaster is also controlled by diffusion transport because of the different dissolution rates at different flow rates. Nevertheless, the dissolution of plaster or gypsum, which is exposed to sodium hydroxide, probably has other mechanisms controlling it. There may be a chemical reaction transforming the surface of plaster.

Figure 4.12 shows the dissolution rate under pH 3, 7 and 10 at the low flow rate. The dissolution rate at pH 10 has highest value at the beginning and decreases until it becomes the lowest value when compared to the other cases. The dissolution rate under pH 3 and 7 are similar until the dissolution rate at pH 3 becomes higher after three hours. This possibly results from the developing of scallops at pH 3 more than at pH 7 and 10 after three hours. This causes the surface area at pH 3 to be higher than at pH 7 and 10.

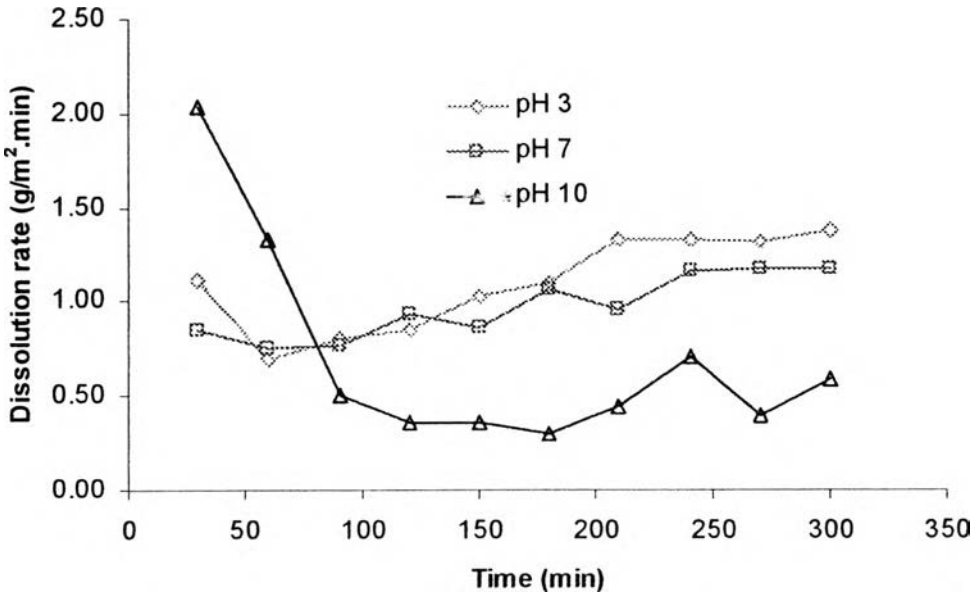

Figure 4.12 Comparison of the dissolution rate at 25 LPM in different pHs

Figure 4.13, it shows the dissolution rate under different pHs at the high flow rate. The dissolution rate at pH 10 is the highest at the beginning of the experiment similar to the dissolution rate at the low flow rate. However, the dissolution rates at the three pHs are similar in value in the range of time between 100 to 160 minutes. After 160 minutes, the dissolution rate at pH 3 and 7 increase until the dissolution rate at pH 3 becomes the highest.

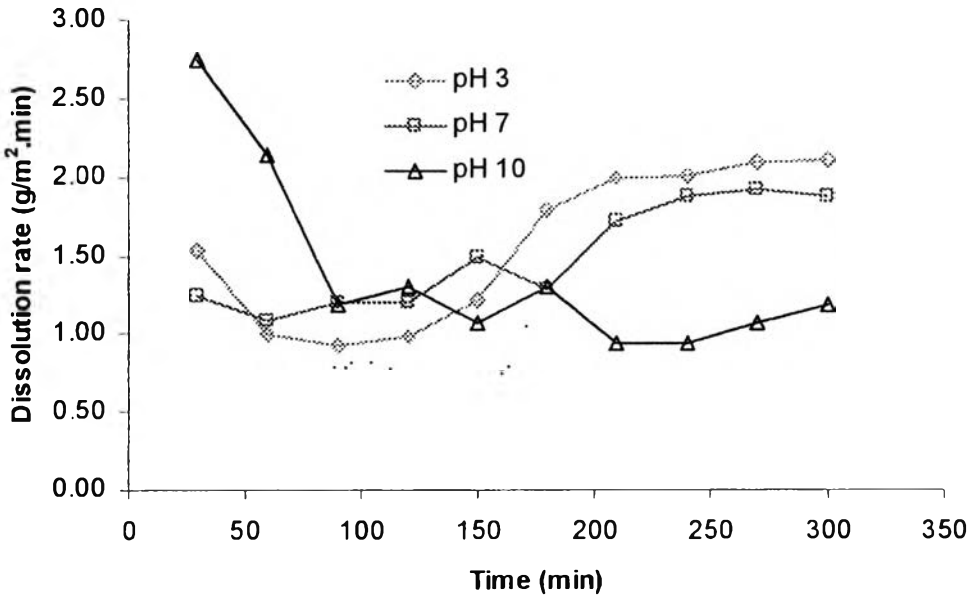

Figure 4.13 Comparison of the dissolution rate at 35 LPM in different pHs

4.3 The Effect Temperature on the Scallop Surface

The two different flow rates and three different pHs were studied at a temperature of 10°C.

4.3.1 Scallop Surface

At 10°C and low flow rate, the formation of scallops is reduced. The population of scallops is small at the three pHs, as shown in Figure 4.14(a1), (b1) and (c1). At the low flow rate, there is little scalloping but at the high flow rate some scallops are formed. Figures 4.14 and 4.15 show a comparison of the population of scallops between low and high temperatures. The population of scallops obviously is

reduced at the low temperature. This indicates that the population of scallops decreases with decreasing temperature and no scallops are formed when the system is operated under the low temperature and the low flow rate. The scallop formation decreases with decreasing the temperature of the fluid.

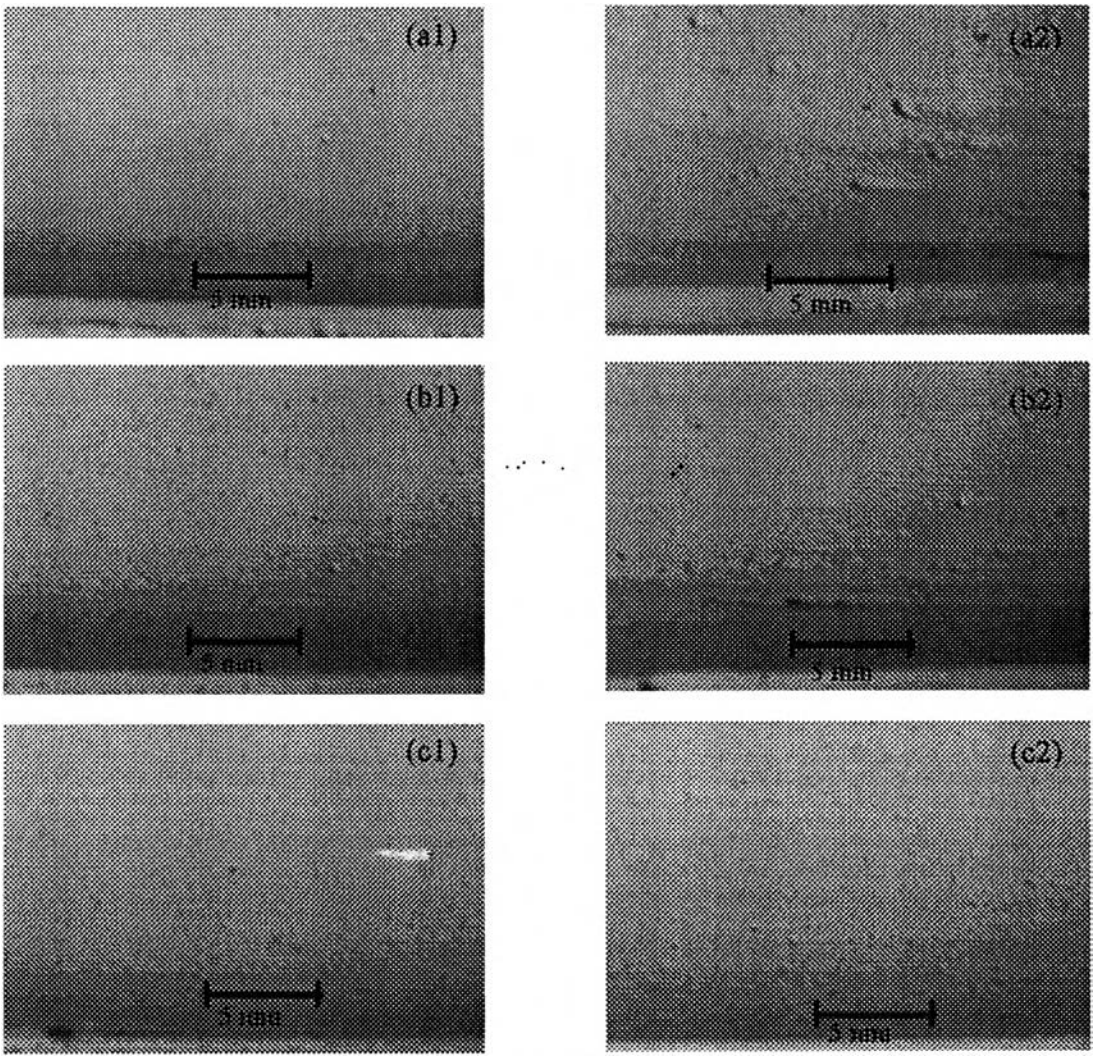

Figure 4.14 Comparison of the scallop surfaces on the plaster surface after run at 25 LPM under different conditions: (a1) $pH_{25°C}$ 3, 10°C, (b1) $pH_{25°C}$ 7, 10°C, (c1) $pH_{25°C}$ 10, 10°C, (a2) $pH_{25°C}$ 3, 25°C, (b2) $pH_{25°C}$ 7, 25°C and (c2) $pH_{25°C}$ 10, 25°C

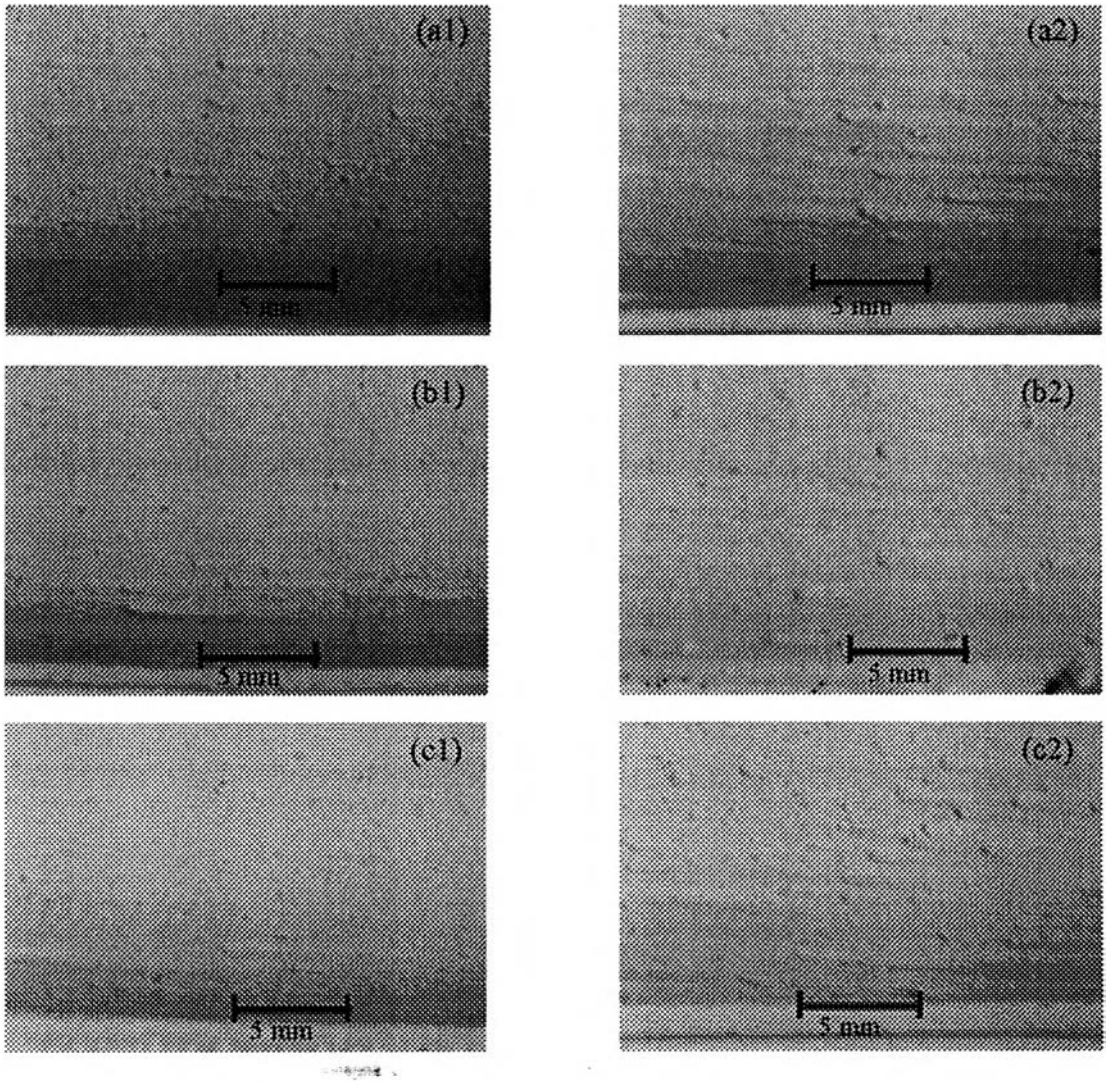

Figure 4.15 Comparison of the scallop surfaces on the plaster surface after run at 35 LPM under different conditions: (a1) $pH_{25°C}$ 3, 10°C, (b1) $pH_{25°C}$ 7, 10°C, (c1) $pH_{25°C}$ 10, 10°C, (a2) $pH_{25°C}$ 3, 25°C, (b2) $pH_{25°C}$ 7, 25°C and (c2) $pH_{25°C}$ 10, 25°C

From observations of scalloping at different times, at low temperature, after the scallops initially form some scallops disappear as the experiment continues, as shown in Figure 4.16. It appears that some scallops disappear if they cannot form larger ones. The scallops at the low temperature are initially formed late compared to the high temperature. Moreover, the scallops are small and less in number. The less

dissolvable plaster affects the initial formation of scallops and the population of scallops.

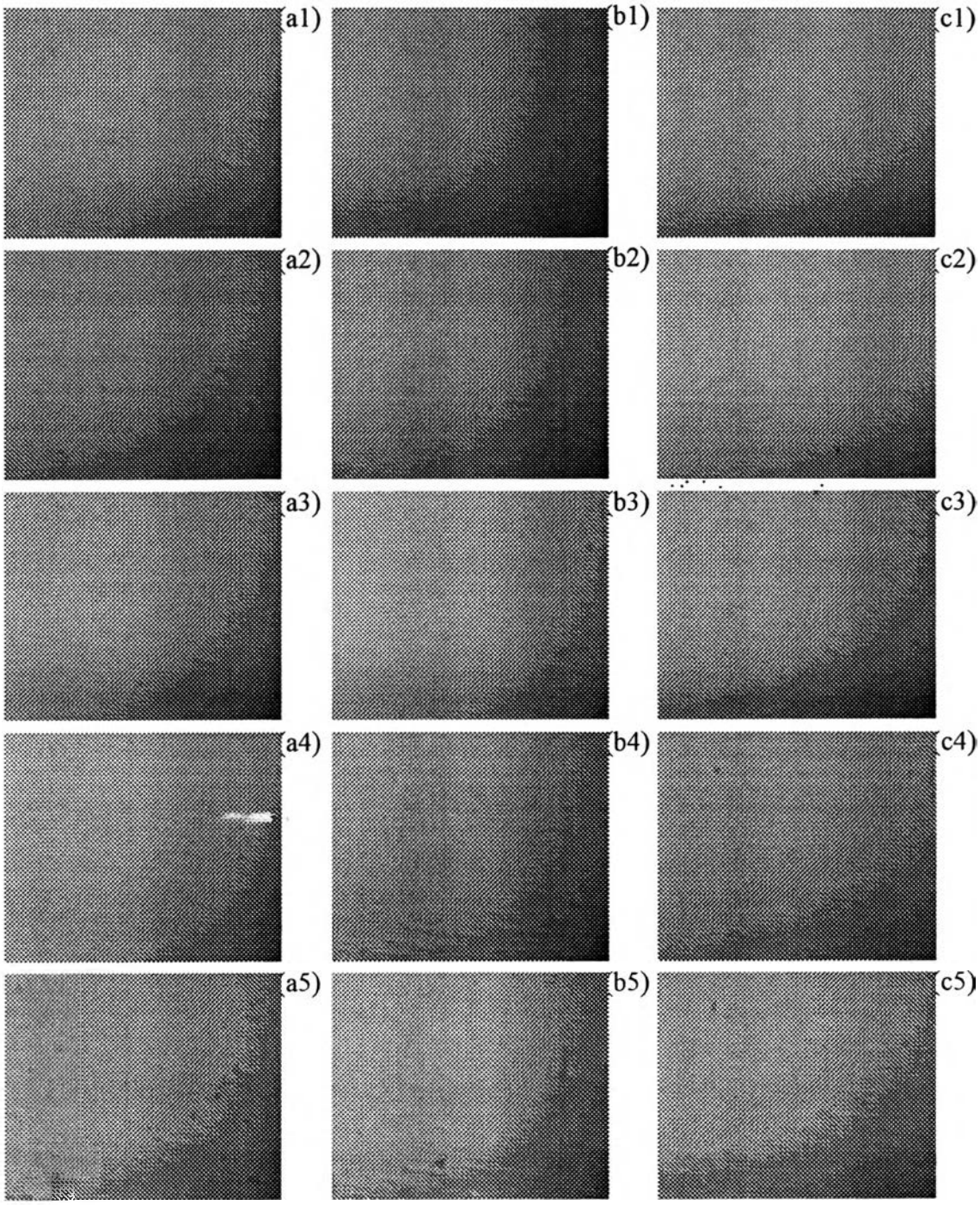

Figure 4.16 The scallop surface developing every one hour at 35 LPM and 10°C under different conditions: (a1-5) $pH_{25°C}$ 3, (b1-5) $pH_{25°C}$ 7 and (c1-5) $pH_{25°C}$ 10

4.3.2 Dissolution Rates

At pH 7 and 10°C, the dissolution rate shows to be stable at the beginning and then increases after 2 hours until it becomes stable after four hours at the high flow rate. However, the dissolution rate is constant at the low flow rate, as shown in Figure 4.17.

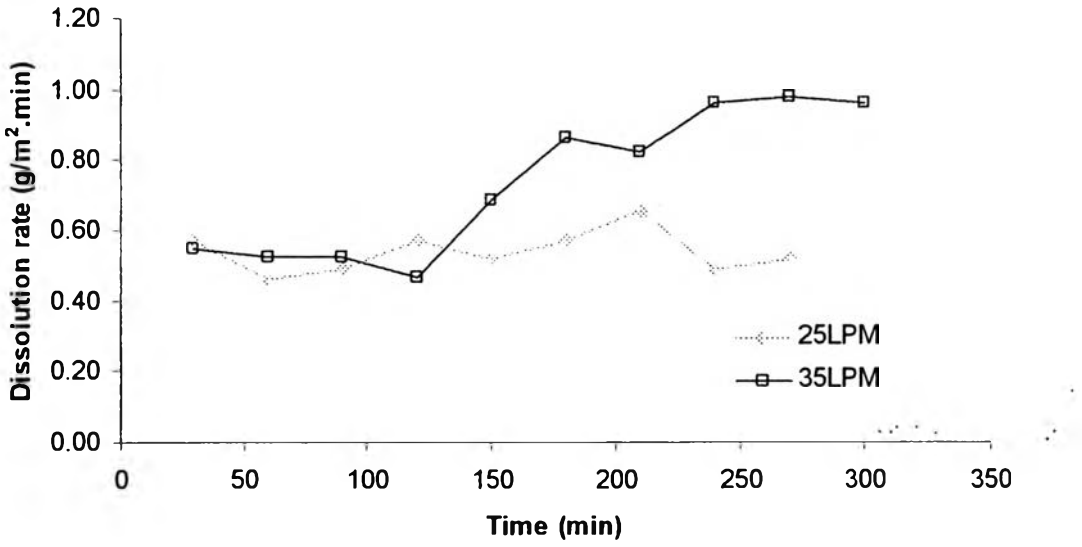

Figure 4.17 The dissolution rate versus time at $pH_{25°C}$ 7, 10°C

At the high flow rate, the dissolution rate is stable initially and increases with time after two hours. This is possibly because the plaster surface is larger after the scallops are formed and this significantly affects the dissolution rate. After four hours, the dissolution rate becomes stable because the pattern of scallops is constant and no more scallops are formed. At the low flow rate, the dissolution rate is nearly constant with time.

At the high flow rate, the dissolution rate is constant at 0.54 $g/m^2.min$ approximately, which is similar to the dissolution rate at the low flow rate. Therefore, it is postulated that the plaster surface is controlled by a surface reaction at the beginning of the experiment. This is possibly because the solubility of the gypsum in pure water decreases with decreasing temperature. After two hours, the dissolution rate of plaster switches from surface reaction control to diffusion transport control as

rate of plaster switches from surface reaction control to diffusion transport control as the experiment proceeds. The mechanisms limiting the kinetic dissolution of plaster may change.

At pH 3 and 10°C, the dissolution rate is high at the beginning of the experiment and decreases with time. At the high flow rate, the dissolution rate increases before it approaches a stable or slightly increasing value after four hours. At the low flow rate, the dissolution rate decreases during the first hour before increasing after 90 minutes, after which it remains stable, as shown in Figure 4.18.

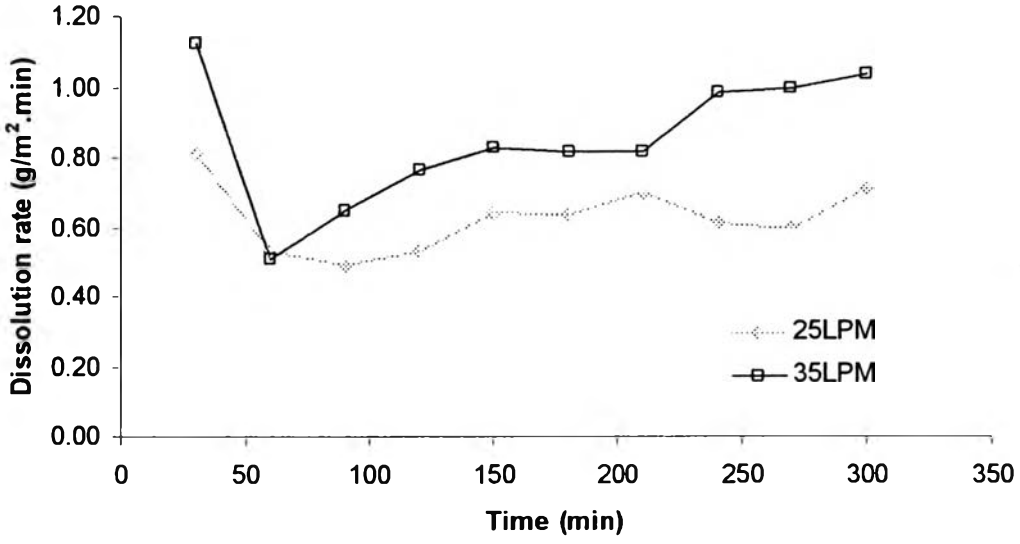

Figure 4.18 The dissolution rate versus time at $pH_{25°C}$ 3, 10°C

For this case, the dissolution rate decreases at the beginning of the experiment and then increases with time similar to the results at the high temperature. It is postulated that the dissolution rate significantly increases with increasing surface area as well.

At the beginning of the experiment, the dissolution rate of plaster is controlled by diffusion transport. As the experiment proceeds, the rate-limiting step for dissolution changes from diffusion transport to surface reaction control for a short period time and then returns to diffusion transport control.

At pH 10 and 10°C, at the high flow rate, the dissolution rate is high at the beginning of the experiment and decreases to approach 0.67 $g/m^2.min$

approximately before it becomes stable at this value after one hour. At the low flow rate, the dissolution rate is high at the beginning of the experiment and then decreases with time before it increases after three hours, as shown in Figure 4.19.

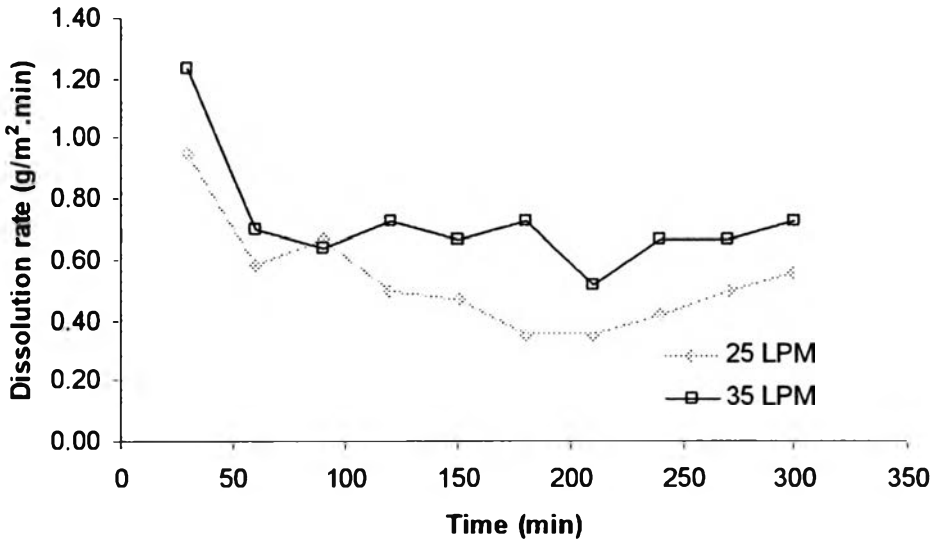

Figure 4.19 The dissolution rate vs time at $pH_{25°C}$ 10, 10°C

The dissolution rate of plaster is controlled by diffusion transport at the beginning of the experiment and then switches to surface reaction control for a short period. However, the diffusion transport is the rate-limiting step at the end of the experiment similar to the result from pH 3 at low temperature.

From Figure 4.20, the dissolution rate profiles are similar in shape at different temperatures but shift down from the high to low temperature. This indicates that the dissolution rate decreases with decreasing temperature but the kinetics of dissolution of plaster are the same. At pH 10 and the low flow rate, however, the dissolution rate is the same after one hour at different temperatures. It is postulated that the temperature has no effect on the dissolution rate at low flow rate for a pH 10.

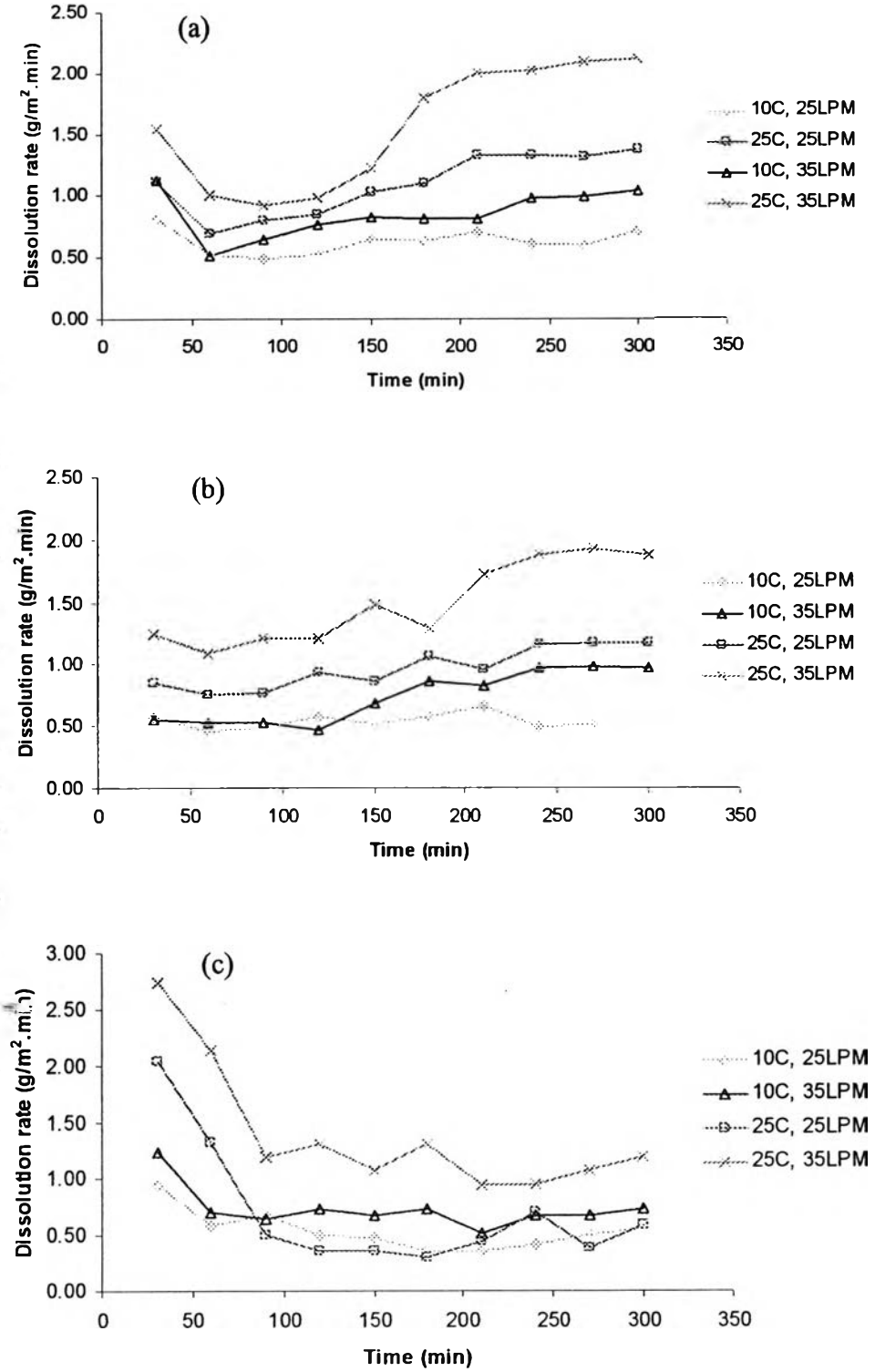

Figure 4.20 Comparison of the dissolution rates under different conditions: (a) $pH_{25°C}$ 3, (b) $pH_{25°C}$ 7 and (c) $pH_{25°C}$ 10

From Figures 4.20(a) and 4.20(b), the dissolution rate at 10°C and 35 LPM is below that at 25°C and 25 LPM. This indicates that the temperature affects the dissolution rate more than the flow rate. This is possible because the temperature can reduce the solubility of the plaster.

In the case of pH 7, the average dissolution rates at room temperature are 0.965 and 1.49 g/m2.min at low and high flow rates, respectively. At 10°C, they are 0.54 and 0.735 g/m2.min at high and low flow rate, respectively. This indicates that the average dissolution rate at room temperature is higher than at the lower temperature by 40-50%. This results from the solubility of plaster at different temperatures, which decreases 7.19% between 25 to 10°C (Azimi *et al*, 2007), see Appendix B. Moreover, the mass transfer coefficient also decreases with decreasing temperature. Therefore, the dissolution rate of plaster is under the mixed kinetics control at the low temperature. From Table 4.1, 4.2 and Figure 4.21, the average dissolution rate decreases very little value when pH decreases but it has more effect on changing temperature. Therefore, it can conclude that the average dissolution rate decreases with decreasing temperature but is little affected by pH.

Table 4.1 The average dissolution rate of plaster from different calculations at 25°C

Solution Condition	The dissolution rate at 25 LPM ($g/m^2 \cdot min$)		The dissolution rate at 35 LPM ($g/m^2 \cdot min$)	
	Weight loss	AAS	Weight loss	AAS
pH 3	1.12	1.10	1.63	1.57
pH 7	1.07	0.97	1.55	1.49
pH 10	1.01	0.90	1.45	1.39

Table 4.2 The average dissolution rate of plaster from different calculations at 10°C

Solution Condition	The dissolution rate at 25 LPM ($g/m^2 \cdot min$)		The dissolution rate at 35 LPM ($g/m^2 \cdot min$)	
	Weight loss	AAS	Weight loss	AAS
pH 3	0.64	0.63	0.89	0.87
pH 7	0.59	0.54	0.80	0.74
pH 10	0.57	0.54	0.75	0.73

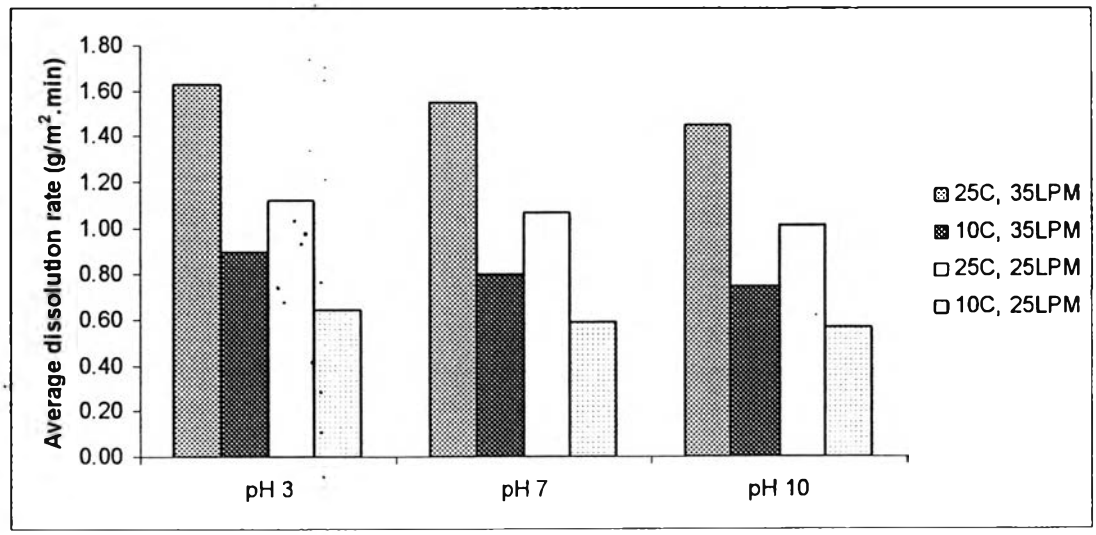

Figure 4.21 Comparison of the average dissolution rates throughout experiment under different conditions.

Berger, et al. mentioned that increasing the sodium hydroxide concentration in the solution will lead to a lower diffusion coefficient. Therefore, it is implied that the average dissolution rate at pH 10 decreases because the mass-transfer coefficient decreases.

From Table 4.1 and 4.2, the average dissolution rates, which were determined by mass variation method and AAS method, show close values each other. The mass variation method confirms the dissolution rate value from AAs method. The deviation of the average dissolution rate between two method is not more than 10%. Therefore, AAS method is a suitable technique to determine the plaster dissolution rates.

4.4 The Other Observation for Understanding the Dissolution Rate Mechanism

Due to the dissolution rate profiles are different in different condition, especially under pH 10. The other analytical techniques were used to determine the plaster surface after run under condition pH 3 and 10.

Moreover, the thickness of plaster was measured so as understand the dissolution rates along the pipe.

4.4.1 Dissolution Rates at pH 3 and 10

From the results at pH 3 (25°C and 10°C), the dissolution rate decreases at the beginning of the experiment. It may be because the plaster surface transformed when the nitric acid solution flow through. From Figure 4.22 and 4.23, the result from analysis the surface from LRS at before run and after run pH 3, it shows that the plaster surface changed. Therefore, it can occur some reaction on the surface and it may result in dissolvable the plaster into the solution, at the beginning of the experiment. However, the solubility of gypsum in nitric acid is so high. The dissolution rate can becomes to increase after a certain time.

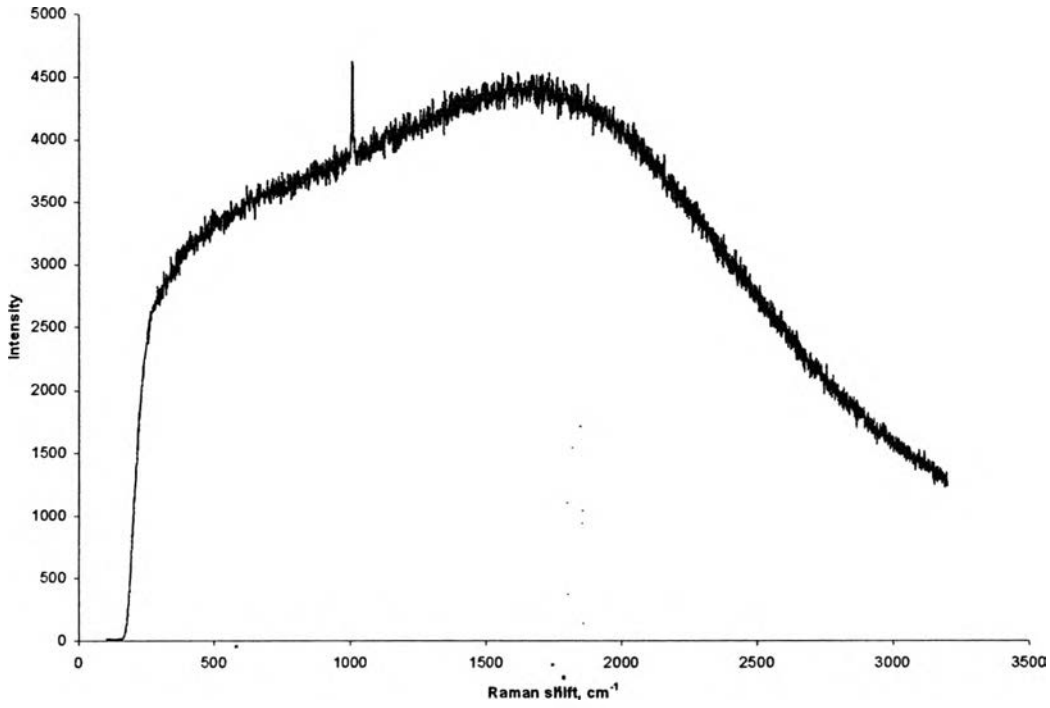

Figure 4.22 Raman spectrum of plaster surface before run

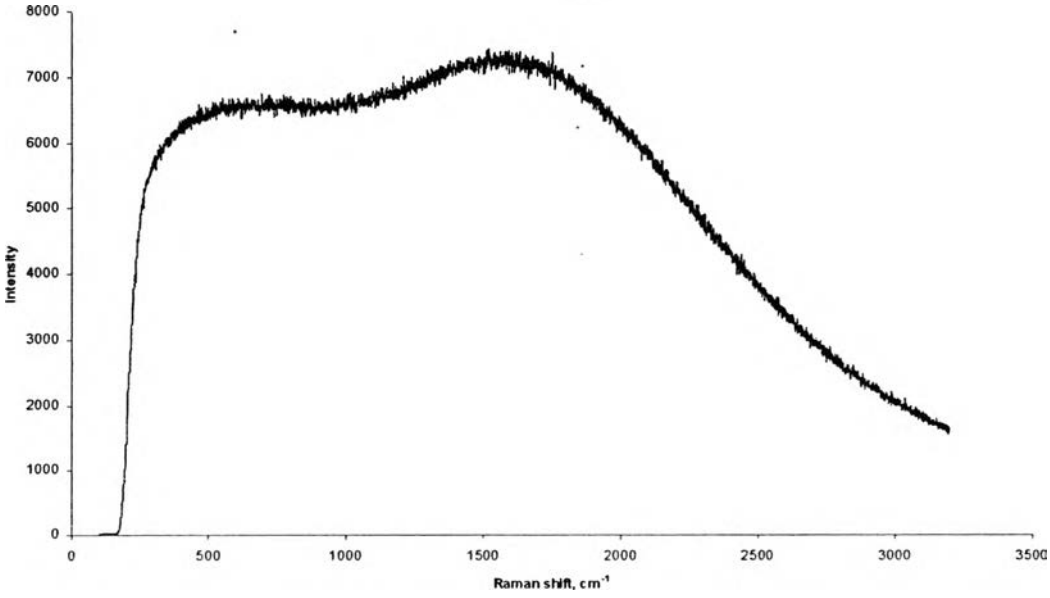

Figure 4.23 Raman spectrum of plaster surface at 25 LPM, $pH_{25°C}$ 3 and 25°C

From the results of pH 10 (25°C and 10°C), the dissolution rate decreases instead of increasing with increasing surface area. In this case, the dissolution rate decreases with time which it is different results from occurring at pH 7 and 3. It postulates that the surface area has less effect on the dissolution rate. From observation on the experiment, it appeared some unknown particles deposit on the sample tubes after run. Therefore, it is possible that the solution reacted the surface and formed the chemical compound to precipitates on the surface and the coated surface becomes insoluble.

For example, Table 4.3 shows the composition of plaster surface at different conditions. At pH 10, the amount of calcium is much more than the other conditions but the sulfate is less. It is possible that the alkaline solution dissolve the sulfate but it is undissolvable the calcium. When the sodium hydroxide solution dissolves the plaster, hydroxide will form with calcium from the plaster and become the calcium hydroxide compound to deposit back on the plaster surface.

$$CaSO_4 + NaOH \longrightarrow \underset{\textit{precipitated}}{Ca(OH)_2} + Na_2SO_4$$

Table 4.3 The composition of plaster after run in different conditions

Condition	Na_2O	MgO	Al_2O_3	SiO_2	SO_3	ClO_0	K_2O	CaO	FeO	Total
Before run	0.21	0.24	0.99	0.35	55.80	0.30	0.11	40.97	1.04	100.00
1	0.14	2.57	1.58	4.08	48.44	0.00	0.48	42.04	0.66	100.00
3	0.32	12.78	1.55	3.71	29.09	0.03	0.62	50.86	1.04	100.00
5	0.14	4.59	2.39	15.44	36.58	0.08	0.75	37.89	2.14	100.00

By comparison of the solubility, it was found that the solubility of calcium hydroxide is lowest when compared with other compounds. The solubility of calcium hydroxide is 1.85 g/l but the solubility of calcium sulfate, sodium hydroxide and sodium sulfate are 2.4, 1110 and 47.6 g/l, respectively. Therefore, it is possible that calcium hydroxide could be deposited when the reaction occurred.

Moreover, Rechenberg and Sprung (1983) found that the calcium content of the solution mainly depends on the alkali. The solubility of calcium decreases if the alkali hydroxide concentration in the solution increases. Therefore, it

is possibly that the calcium be less dissolved in the sodium hydroxide solution as the process proceeds.

Other mechanisms may also be involved in the decrease of plaster dissolution rate with time. For example, there might be a chemical reaction transforming the surface of the plaster. Figure 4.22 and 4.24 show the results from using the LRS at before run and after run pH 10. At pH 10, it has no peak but there is one peak at pH 3 and 7. It postulates that the plaster surface is transformed when it is flowed with alkaline solution.

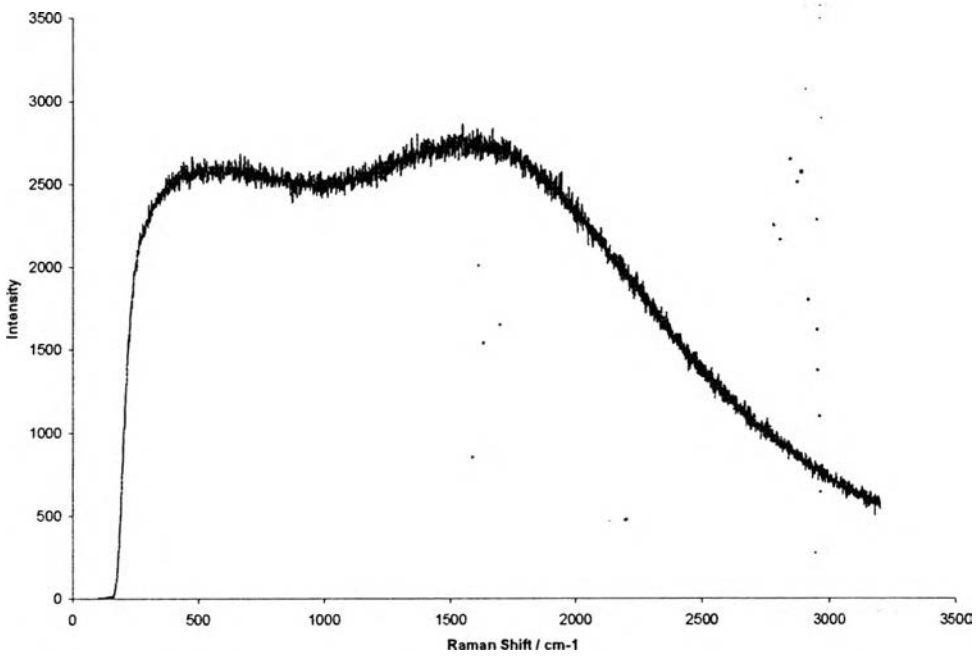

Figure 4.24 Raman spectrum of plaster surface at 25 LPM, $pH_{25°C}$ 10 and 25°C

4.4.2 Dissolution Rates Along the Pipe

The plaster pipes were measured for thickness every centimeter along the 75 cm long half-cylinder. These measurements were used to calculate the dissolution rates and obtained the dissolution rates along the pipe at different conditions, as shown Figure 4.25 to 4.30 (see more results in Appendix F). They show the dissolution rates are high at the inlet of the pipe (upstream) and

substantially decreases and then increase before decreasing at the outlet of the pipe (downstream).

This indicates that the dissolution rates are high at the inlet. The diameter connection between the main pipe and the test section changes some what between the pipes. The dissolution rates decrease downstream because the plaster dissolves to the bulk and the solution becomes more saturated with plaster giving less driving force. Therefore, it causes the plaster to be less dissolvable downstream.

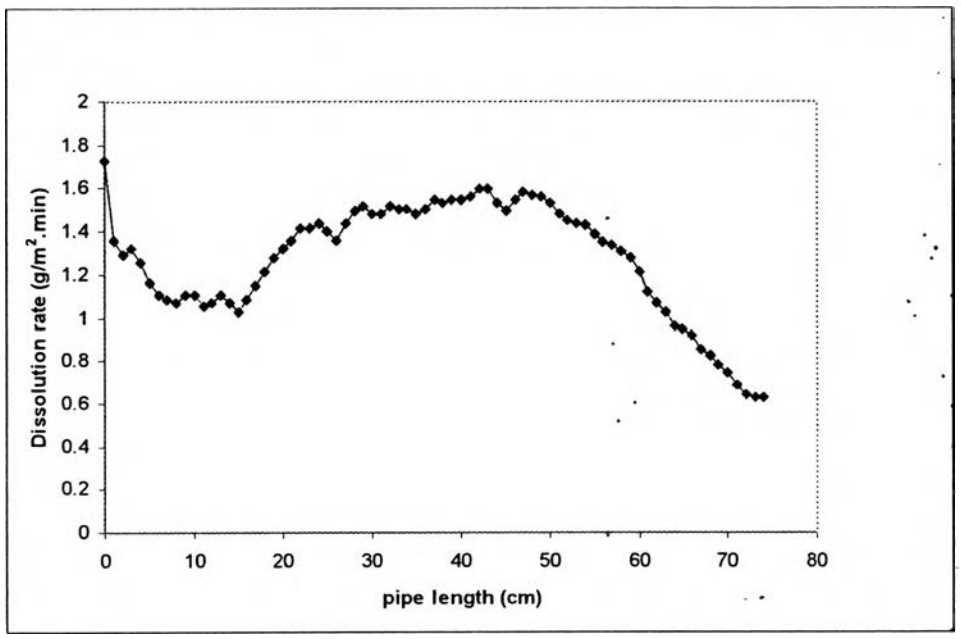

Figure 4.25 The dissolution rate profile along the pipe under condition $pH_{25°C}$ 3, 25°C and 25 LPM

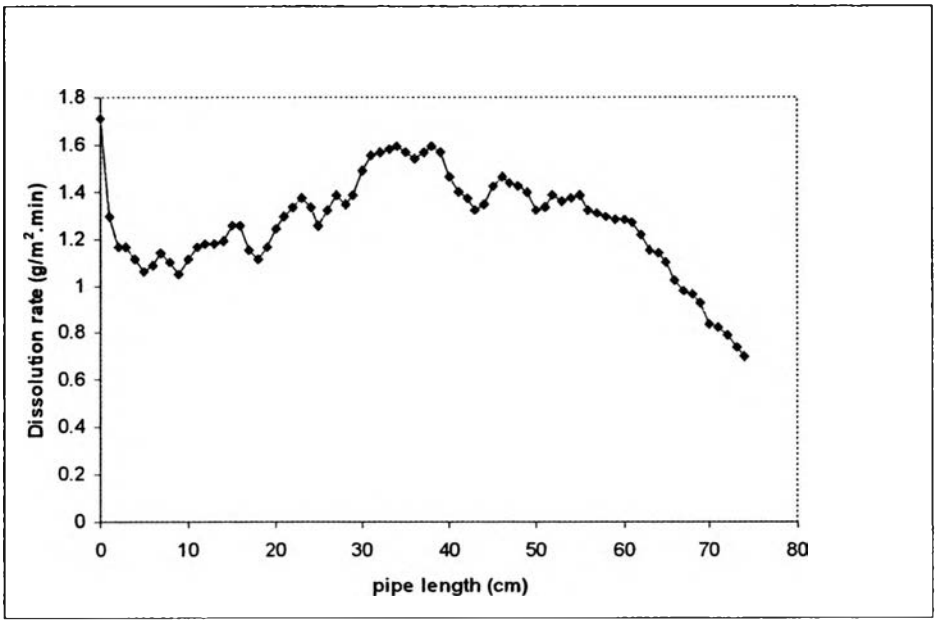

Figure 4.26 The dissolution rate profile along the pipe under condition $pH_{25°C}$ 7, 25°C and 25 LPM

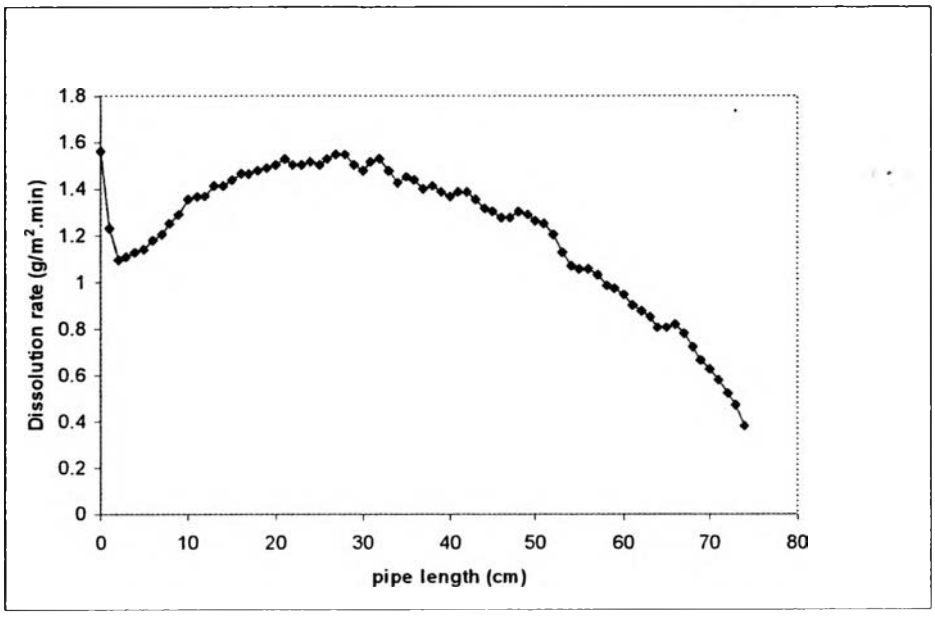

Figure 4.27 The dissolution rate profile along the pipe under condition $pH_{25°C}$ 10, 25°C and 25 LPM

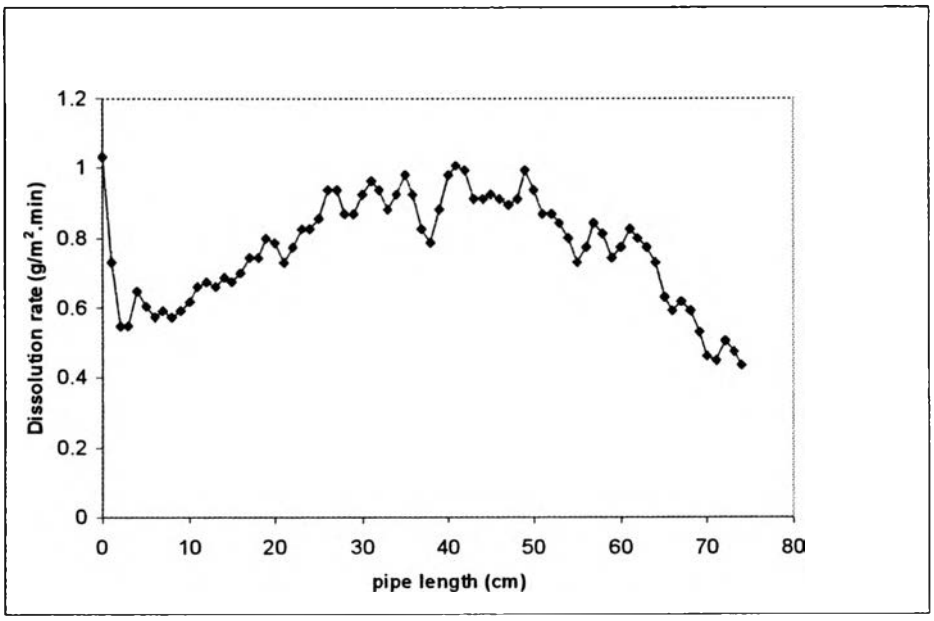

Figure 4.28 The dissolution rate profile along the pipe under condition $pH_{25^{\circ}C}$ 3, 10°C and 25 LPM

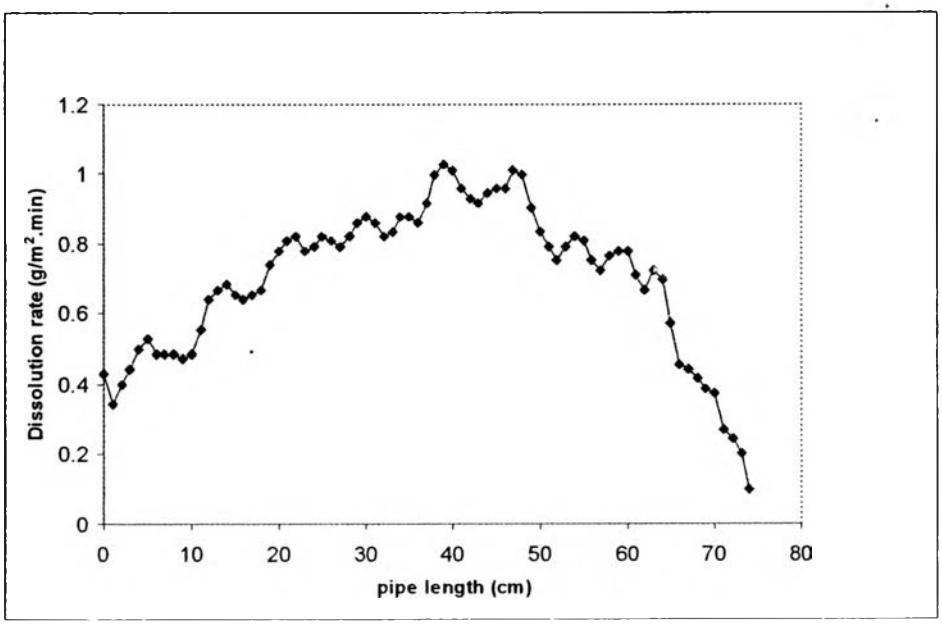

Figure 4.29 The dissolution rate profile along the pipe under condition $pH_{25^{\circ}C}$ 7, 10°C and 25 LPM

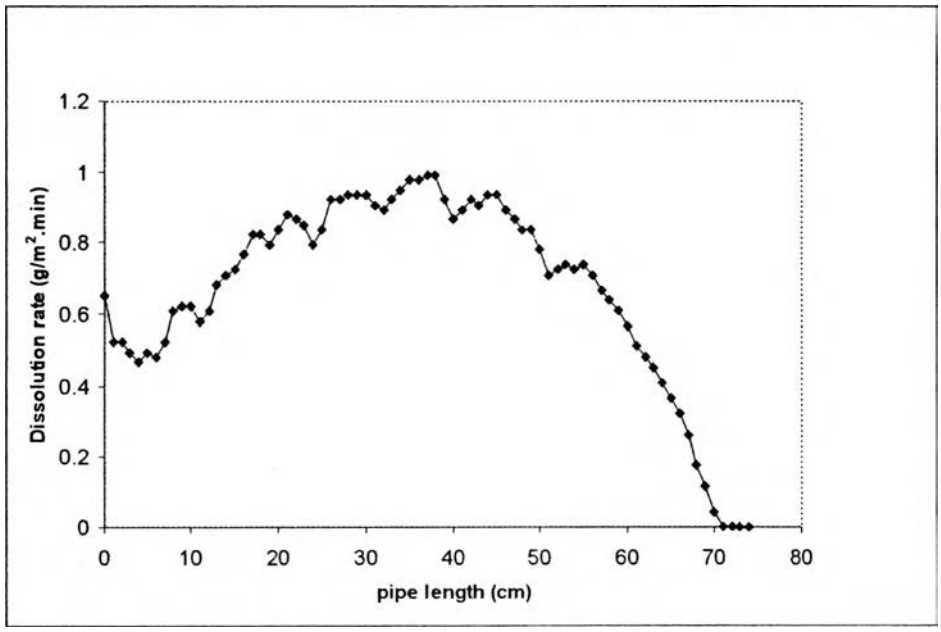

Figure 4.30 The dissolution rate profile along the pipe under condition $pH_{25°C}$ 10, 10°C and 25 LPM

4.4.3 Dissolution Coefficient Along the Pipe

The rate constants were determined from the dissolution rates along the pipe. The rate constants at each distance of the pipe called "the dissolution coefficient" were determined. Figures 4.31 to 4.36 show the dissolution coefficients under different conditions, see more results in Appendix F. The dissolution coefficient profiles are similar to the dissolution rate profile, as above, because the dissolution coefficients were calculated from the dissolution rates along the pipe. Moreover, the mass transfer coefficient was calculated from the operating conditions and compared to the dissolution coefficient. It was found that the mass transfer coefficients were closed to the dissolution coefficients. This confirms that the diffusion transport is the major mechanism in the plaster or gypsum dissolution, as mention above.

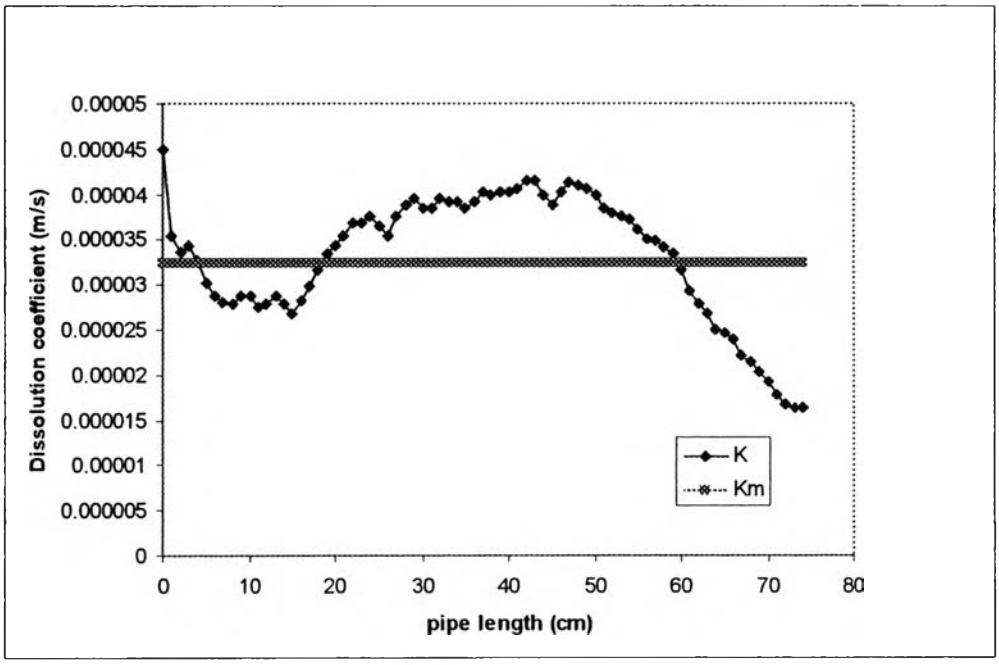

Figure 4.31 The dissolution coefficient (K) compared with the mass transfer coefficient (K_m) along the pipe under condition $pH_{25°C}$ 3, 25°C and 25 LPM

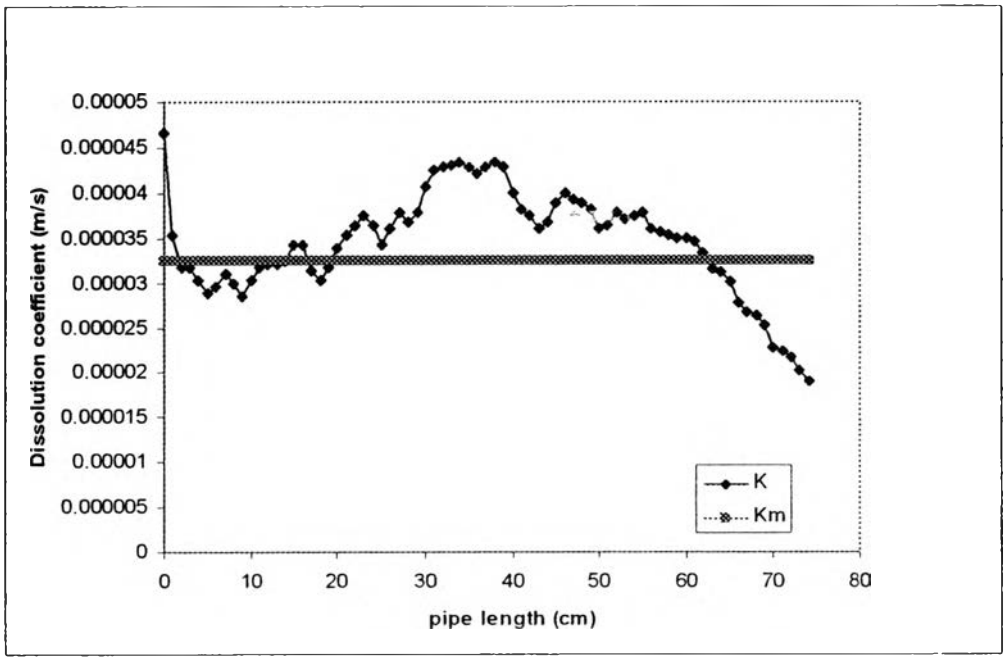

Figure 4.32 The dissolution coefficient (K) compared with the mass transfer coefficient (K_m) along the pipe under condition $pH_{25°C}$ 7, 25°C and 25 LPM

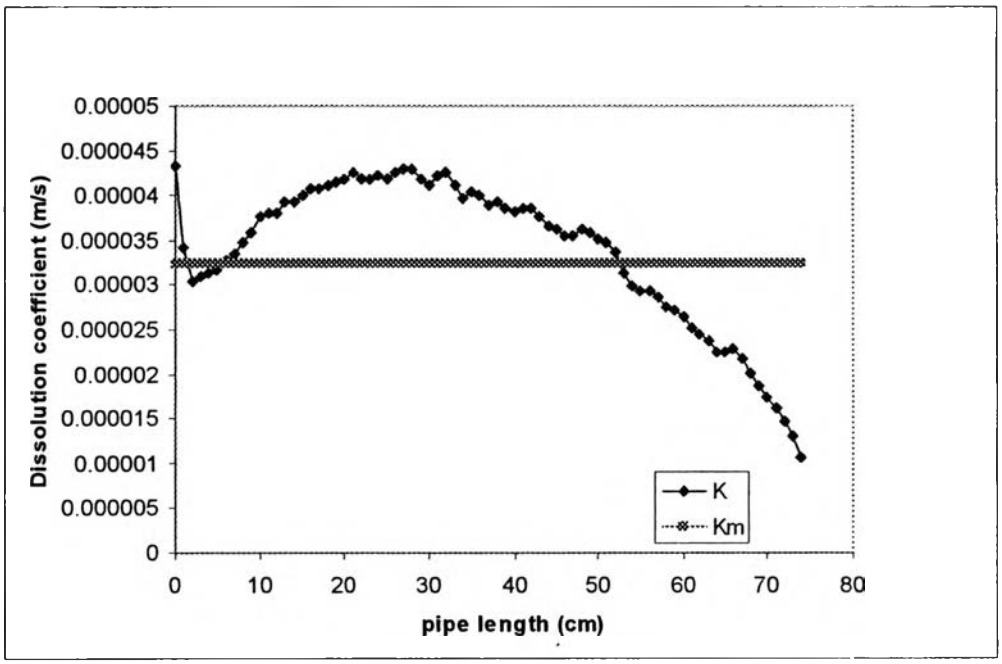

Figure 4.33 The dissolution coefficient (K) compared with the mass transfer coefficient (K_m) along the pipe under condition $pH_{25°C}$ 10, 25°C and 25 LPM

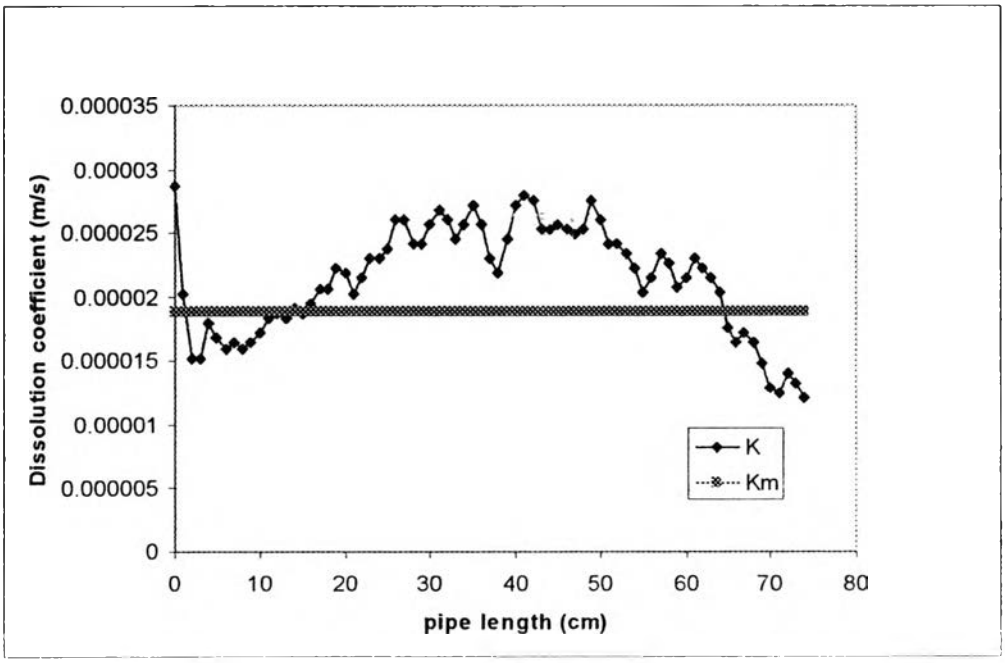

Figure 4.34 The dissolution coefficient (K) compared with the mass transfer coefficient (K_m) along the pipe under condition $pH_{25°C}$ 3, 10°C and 25 LPM

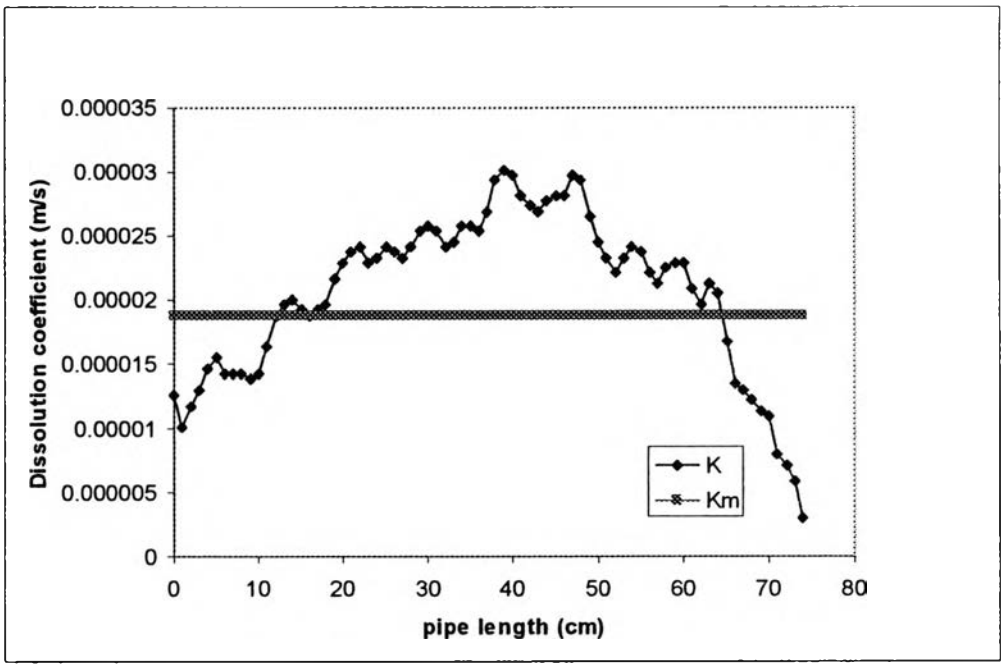

Figure 4.35 The dissolution coefficient (K) compared with the mass transfer coefficient (K_m) along the pipe under condition $pH_{25°C}$ 7, 10°C and 25 LPM

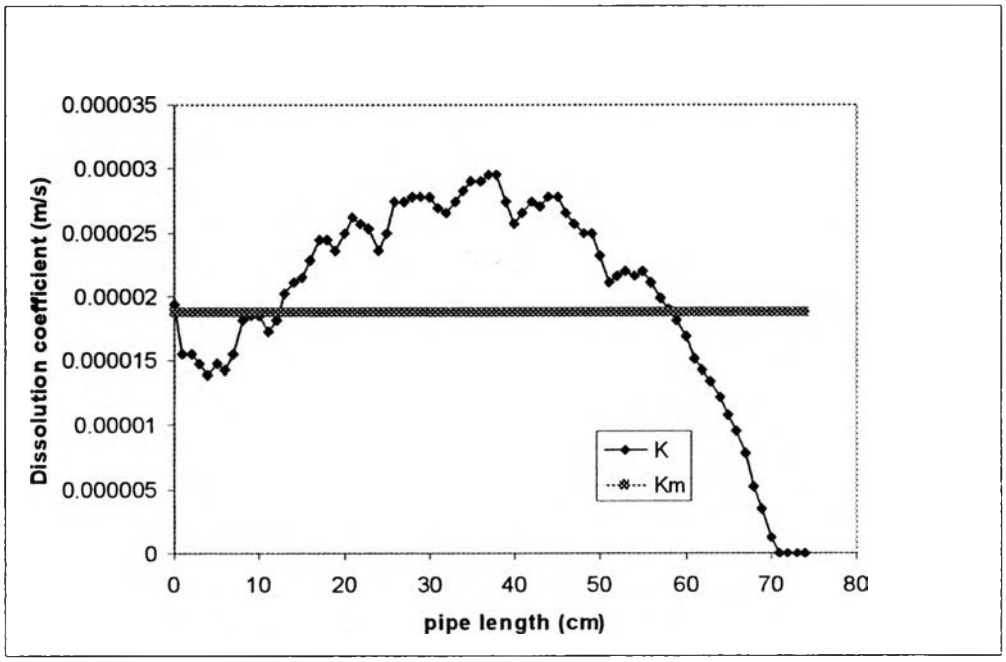

Figure 4.36 The dissolution coefficient (K) compared with the mass transfer coefficient (K_m) along the pipe under condition $pH_{25°C}$ 10, 10°C and 25 LPM